Time scales for transition in Taylor-Couette flow

Olivier Czarny
Association Euratom-CEA, CEA Cadarache, 13108 Saint-Paul-lez-Durance Cedex, France and MSNM-GP, CNRS-Universités d'Aix-Marseille, IMT, La Jetée-Technopôle de Château-Gombert, 38 rue Frédéric Joliot-Curie, 13451 Marseille Cedex 20, France

Richard M. Lueptow[a)]
Northwestern University, 2145 Sheridan Road, Evanston, Illinois 60201

(Received 8 December 2006; accepted 8 March 2007; published online 8 May 2007)

The time scale for onset and decay of vortices in a Taylor-Couette system cannot be predicted from linear stability analysis, yet it is important from a practical standpoint. A two-dimensional pseudospectral direct numerical simulation was used to examine the time scales for subcritical-to-supercritical transition and supercritical-to-subcritical transition for a variety of aspect ratios ($\Gamma=H/d=8,16,24,32,40,\infty$) and radius ratios ($\eta=0.5$, 0.7, and 0.9). A viscous time scale incorporating both the gap width, d, and the distance between the endwalls of the system, H, is most appropriate for the onset of Taylor vortices, although no time scale collapses the data for all aspect ratios and radius ratios. For decay, a viscous time scale using the gap width as the length scale collapses the data as the aspect ratio gets large. These results indicate that the onset of vortices is a consequence of the propagation of vortical structures related to the endwalls, while decay is related to viscous dissipation from the sidewalls. © *2007 American Institute of Physics*.
[DOI: 10.1063/1.2728785]

I. INTRODUCTION

The Taylor-Couette system of shear flow between a rotating inner cylinder and a concentric, fixed outer cylinder provides valuable insight into linear stability and low-dimension bifurcation phenomena. Our interest here is in the time that it takes for the onset and decay of the supercritical Taylor vortex structure. Taylor's original linear stability analysis based on infinitely long cylinders gives no clue about the time scale for the appearance of the vortical structure—the vortices should appear instantaneously for a supercritical Taylor number, and the subcritical to supercritical transition is ideally described by a pitchfork bifurcation. However, the imposition of the no-slip boundary condition at the endwalls results in the pressure gradient force not being balanced by the local centrifugal forces. This induces a vortex or series of vortices, sometimes called Ekman vortices,[1–4] that are unrelated to the centrifugal Taylor instability. These endwall effects can penetrate the entire flow, because of the elliptic nature of the equations of motion,[5] though the strength of the vortices decays with distance from the endwalls.[3,4] The Ekman vortices upset the normal pitchfork bifurcation leading to one branch having a continuous transition from a featureless stable flow to a vortical flow.[1–4,6–9] When Taylor vortices occur, their sense of rotation is controlled by the original Ekman vortices, even for relatively long cylinders[10] (although anomalous rotation can be forced under some conditions for very short or instantaneously started systems[11–14]). However, the Ekman vortices affect the speed with which Taylor vortices appear as the front of the axially periodic vortical state propagates away from the endwalls into the stable cylindrical Couette flow.[2,3,15]

There are several reasonable time scales that could be considered for Taylor vortex flow to become fully developed. The Rayleigh problem suggests a viscous time scale $\tau_v=L^2/\nu$, where L is a characteristic length scale, ν is the kinematic viscosity, and the v subscript on τ indicates a viscous time scale. For infinitely long cylinders, the only characteristic length scale is the radial gap $d=r_o-r_i$ between cylinders of radius r_i and r_o. This leads to a time scale that has been frequently considered,[2,15–27] $\tau_{v,r}=d^2/\nu$, where the r subscript indicates the radial length scale, or variations $(2d)^2/\nu$ and $d^2/2\pi\nu$.[3,28] From a practical standpoint, an experimental apparatus always has finite length, H, leading to a second viscous time scale $\tau_{v,z}=H^2/\nu$,[16,17,20] where the z subscript indicates the axial length scale. In most Taylor-Couette flow experiments, $\Gamma=H/d$ is intentionally large, so $\tau_{v,r}\ll\tau_{v,z}$. A mixed time scale based on both H and d, $\tau_{v,m}=Hd/\nu$, has also been used,[17,29–31] where the m subscript indicates a mixed time scale. Finally, a fourth time scale is based *directly* on the characteristic time scale for spin-up of a fluid between a pair of rotating disks, $\tau_s=\mathrm{Ek}^{1/2}\Omega^{-1}$, where $\mathrm{Ek}=\nu/\Omega L^2$ is the Ekman number, and Ω is the rotational speed.[32] Using the distance between the two endwalls (the rotating disks), H, as the characteristic length scale, the spin-up time scale is $\tau_s=H/(\nu\Omega)^{1/2}$.[16,18]

Our goal is to determine which of these time scales describes the transition from subcritical to supercritical Taylor-Couette flow (onset) and vice versa (decay). This goal can be rephrased as follows: Do the viscous effects propagate from the sidewalls ($\tau_{v,r}$ is the appropriate time scale), from the endwalls ($\tau_{v,z}$ is the appropriate time scale), from a combination of these two effects ($\tau_{v,m}$ is the appropriate time

[a)]Author to whom correspondence should be addressed. Electronic mail: r-lueptow@northwestern.edu

scale), or as a spin-up or spin-down between the endwalls (τ_s is the appropriate time scale)? Furthermore, do the time scales reflect mechanisms for the onset transient that are different from those for the decay transient?

A variant on this problem was addressed recently by Abshagen *et al.*[9] and Manneville[33] in terms of the time scales based on the Landau amplitude theory and the Ginzburg-Landau equation. This approach, while worthwhile, can lead to some unusual results. For example, Abshagen *et al.* found that the Landau time constant based on fitting to experimental time series is much longer for decay than for onset (their Fig. 3). Yet, experimental and numerical time series show the opposite (their Figs. 1 and 4). Another challenge is that the perfect character of the bifurcation represented by the Landau equation cannot account for the altered bifurcation resulting from physical no-slip boundary conditions at the endwalls of an experimental Taylor-Couette cell.

Here, we adopt a pragmatic approach that complements this recent work.[9,33] We simply consider both onset and decay for Taylor-Couette flow at various aspect ratios, $\Gamma = H/d$, and radius ratios, $\eta = r_i/r_o$, and compare the time for the flow to adjust to an abrupt change in terms of the various dimensionless time scales ($\tau_{v,r}$, $\tau_{v,z}$, $\tau_{v,m}$, or τ_s) to determine the appropriate time scale. Of course, this scale also reflects the physical mechanisms for onset or decay.

II. GEOMETRY AND NUMERICAL METHOD

We consider axisymmetric Couette flow in an annular cavity with a fixed outer cylinder and the inner cylinder rotating at Ω_i to provide a Reynolds number $\mathrm{Re} = \Omega_i r_i d/\nu$. The incompressible Navier-Stokes equations with fixed endwall boundary conditions were solved using a pseudospectral Chebyshev collocation direct numerical simulation method[34] identical to that used our previous work,[4,35] including combined backward implicit Euler, explicit Adams Bashforth, and fully implicit schemes for time discretization,[36] along with a projection algorithm for velocity-pressure coupling.[37] Results based on the method are in good agreement with theory[38,39] and measurements,[8] as described previously.[4] The two-dimensional grid had $M = 151-351$ points in the axial direction, depending on Γ, and $N = 31$ points in the radial direction to fully resolve the vortical structure and boundary layers at the endwalls.

The simulation was performed for aspect ratios of $\Gamma = 8$, 16, 24, 32, and 40 (corresponding to $M = 151$, 201, 251, 301, and 351) for a radius ratio of $\eta = 0.5$ and for $\Gamma = 8$, 16, and 32 ($M = 151$, 201, and 301) for radius ratios of $\eta = 0.7$ and 0.9. To model transition to vortical flow, the simulation was initiated at $\varepsilon = \mathrm{Re}/\mathrm{Re}_{\mathrm{crit}} = 0.9853$, and then a step increase in Reynolds number to $\varepsilon = 1.0073$ was imposed. (The critical Reynolds number, $\mathrm{Re}_{\mathrm{crit}}$, was based on the results of DiPrima *et al.*[38]) Likewise, decay from vortical to nonvortical flow was modeled by a step decrease from $\varepsilon = 1.0073$ to 0.9853. In addition, an infinitely long annulus ($\Gamma = \infty$) was simulated using a traction-free endwall boundary condition for $\Gamma = 8$ ($M = 151$) and $\eta = 0.5$ (though the axial wavelength for the vortices was forced to be $2d$). In all cases, the axial profile of the radial velocity v_r halfway across the annular gap (midgap) was recorded as a function of time to track the existence and strength of the vortical structure.

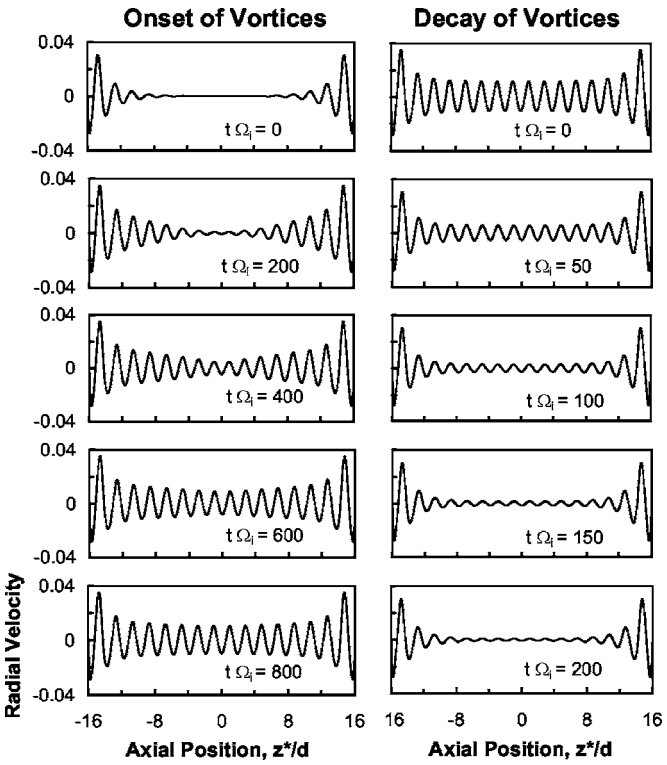

FIG. 1. An example of onset and decay based on the dimensionless radial velocity midway between the inner and outer cylinders for $\Gamma = 32$ and $\eta = 0.7$. Each peak corresponds to a vortex pair. The initial condition at the instant the step change in ε is imposed corresponds to $t\Omega_i = 0$. The time increments are four times longer for onset than for decay.

III. ONSET AND DECAY OF TAYLOR VORTICES

Consider first the transition from stable circular Couette flow ($\varepsilon = 0.9853$) to Taylor vortex flow ($\varepsilon = 1.0073$), shown in the left column of Fig. 1 (onset of vortices) for $\Gamma = 32$ and $\eta = 0.7$. In this figure, the dimensionless radial velocity $v_r/\Omega_i r_i$ midway between the inner and outer cylinders is plotted along the length of the annulus, z^*. Maxima correspond to outflow regions, and minima correspond to inflow regions, so that a vortex pair occurs between any adjacent pair of maxima or minima. For the initial condition corresponding to the instant when the step increase in ε is imposed ($t\Omega_i = 0$), Ekman pumping induces a strong endwall vortex near each endwall. Radial inflow and outflow regions appear at several adjacent induced vortex pairs, but the strength of the vortices decays with distance from the endwalls.[3] These are not Taylor vortices, since they are not driven by a centrifugal instability. As time progresses, the endwall vortices remain nearly the same, but adjacent vortices grow in strength and new vortices appear toward the midlength of the annulus due to the centrifugal instability, consistent with previous results,[3,4,7–9,15] until the vortical structure reaches its full strength at $t\Omega_i = 800$.

The decay of the Taylor vortex structure from $\varepsilon = 1.0073$ to 0.9853 is quite different, as shown in the right column of Fig. 1 with time reset to zero for the instant that

TABLE I. Time ($t\Omega_i$) to achieve 95% of the change from the initial value of the maximum inward radial velocity at midgap to the final value for onset and decay.

	η=0.5		η=0.7		η=0.9	
Γ	Onset	Decay	Onset	Decay	Onset	Decay
8	219	175	103	88	44	39
16	735	364	372	187	151	82
24	1140	444	—	—	—	—
32	1390	473	835	235	384	102
40	1590	483	—	—	—	—
∞	8440	485	—	—	—	—

the step decrease in ε is imposed. The Taylor vortices decay nearly uniformly along the length of the annulus (except near the endwalls), consistent with previous simulations.[9] In addition, the time scale for onset is several times that for decay. For lower aspect ratios Γ, the time for onset is only slightly longer than that for decay due to the influence of the Ekman endwall vortices, as indicated in Table I. As the aspect ratio increases, the time for onset can be several times that for decay. For the infinitely long cylinder, $\Gamma=\infty$, the time for onset is more than an order of magnitude longer than the time for decay. Furthermore, for $\eta=0.5$, the time for decay asymptotes to $t\Omega_i \approx 485$ as the aspect ratio increases, whereas the time for onset does not seem to have an asymptotic character.

IV. TIME SCALE FOR ONSET AND DECAY OF TAYLOR VORTICES

The task at this point is to determine which of the nondimensional time scales properly scales the transition (either onset or decay) and thus reflects the physics of the transition. To do this, we consider the time record of the maximum radial inflow velocity v_r' at midgap and approximately midlength and nondimensionalize the time with each of the four proposed time scales: $\tau_{v,r}=d^2/\nu$, $\tau_{v,z}=H^2/\nu$, $\tau_{v,m}=Hd/\nu$, or $\tau_s=H/(\nu\Omega)^{1/2}$. Because the magnitudes of the radial inflow velocities differ, particularly as the radius ratio changes, the radial velocity for onset is normalized as $V_r=(v_r'-v_{r,0}')/(v_{r,\infty}'-v_{r,0}')$, where $v_{r,0}'$ is the initial velocity at $t=0$, and $v_{r,\infty}'$ is the steady-state velocity as $t\to\infty$. Using this scaling, the normalized velocity varies between 0 and 1. Figure 2 displays the time record for the computational scaling ($t\Omega_i$) and the four proposed time scales for $\eta=0.5$. From the computational scaling in Fig, 2(a), it is quite clear that it takes longer for the radial velocity to reach steady state as the length of the annulus increases. For comparison, for the case of a traction-free endwall condition, $\Gamma\to\infty$, the time to transition is $t\Omega_i \sim 8000$, an order of magnitude longer than that for the finite geometries.

Figures 2(b)–2(e) plot the same data using the four proposed time scales. Clearly, the data do not collapse for any of the time scales. Using the time scale based on the distance between the endwalls, $\tau_{v,z}=H^2/\nu$, results in the curves overlapping the initial portion of the onset, but does not collapse the data after the velocity reaches about one-half of its final velocity. On the other hand, using the mixed time scale, $\tau_{v,m}=Hd/\nu$, or the spin-up time scale, $\tau_s=H/(\nu\Omega)^{1/2}$, results in overlap of the curves after the velocity reaches about 75% of its final value when the case of $\Gamma=8$ is excluded (most likely because of the strong effect of the endwall Ekman vortices in this case). Two different time scales for onset are consistent with the idea[33] that the early stage is related to front propagation,[2,3,15] while the later stage is slow convergence of the solution to its final shape via a phase-diffusion process, at least for large aspect ratios ($\Gamma>16$).[33] From Figs. 2(c)–2(e), it appears that the time for front propagation scales with a viscous time scale related to the distance between the endwalls, while the slow diffusive relaxation to the final solution is related either to the combined effect of the endwalls and sidewalls (the mixed time scale) or to the spin-up of the system.

The situation is quite different for decay from supercritical to subcritical flow, as indicated in Fig. 3. Here, the radial velocity is normalized as $V_r=(v_r'-v_{r,\infty}')/(v_{r,0}'-v_{r,\infty}')$, so V_r starts at 1 and decays to zero. The computational scaling [Fig. 3(a)] results in near-collapse of the data for all aspect ratios including the traction-free endwall condition (not shown in the figure), except $\Gamma=8$, where endwall effects play a large role. The time scale based on the gap width, shown in Fig. 3(b), collapses the data, as would be expected for a single radius ratio, but none of the time scales that include the distance between the endwalls are as effective. These results point to viscous effects between the walls of the two cylinders separated by d controlling the decay of the vortical structure.

Of course, the only way to test these conclusions is to vary the gap width, so we consider radius ratios $\eta=0.7$ and 0.9 for $\Gamma=8$, 16, and 32, as well as $\eta=0.5$ in Fig. 4. Several results are evident. First, none of the proposed time scales collapse the data for all radius ratios and all aspect ratios. In Fig. 4(a) for $\tau_{v,a}=d^2/\nu$, the data for all three radius ratios collapse onto single curves for $\Gamma=8$ and 16, but they do not collapse for $\Gamma=32$, indicating that the endwalls control the onset of vortical motion, particularly for small aspect ratios. This is confirmed by the collapse of the data for $\Gamma=8$ and 16 for the entire transient using $\tau_{v,z}=H^2/\nu$ in Fig. 4(b). This time scale does not work as well for larger aspect ratios, because the endwalls (and the Ekman vortices associated with them) exert less control over the onset of vortical mo-

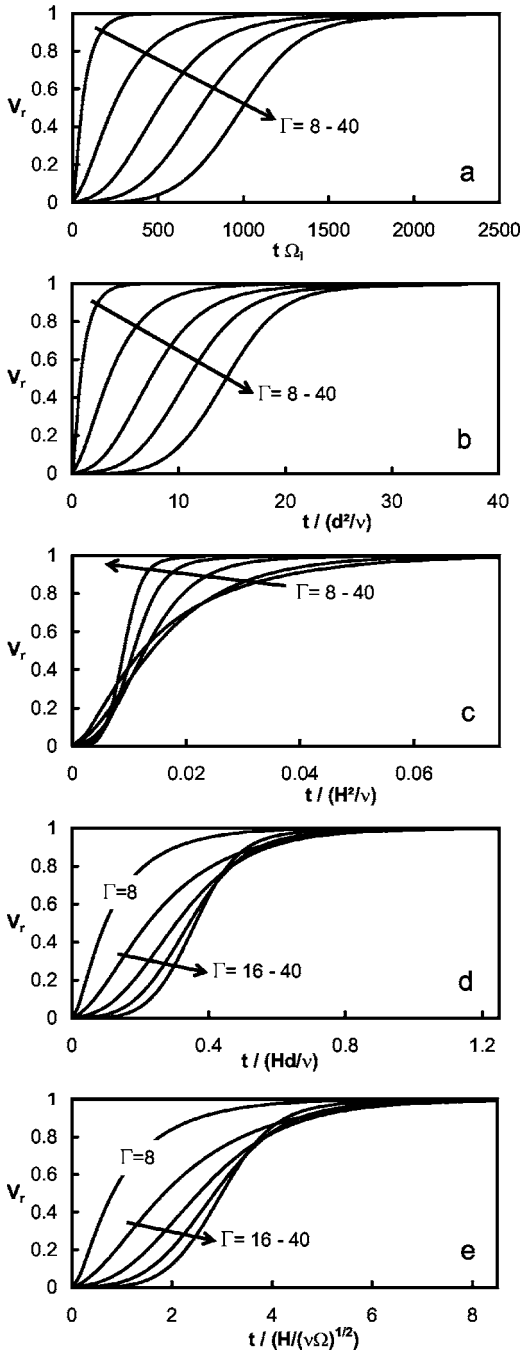

FIG. 2. Onset transient of the normalized maximum radial velocity for $\Gamma=8,16,24,32,40$ and $\eta=0.5$. (a) Time is scaled as $t\Omega_i$ based on the native computational scale; (b) time is scaled as $t/(d^2/\nu)$ using a viscous time scale based on the gap between the cylinders; (c) time is scaled as $t/(H^2/\nu)$ using a viscous time scale based on the distance between the endwalls; (d) time is scaled as $t/(Hd/\nu)$ using a mixed viscous time scale; (e) time is scaled as $t/[H/(\nu\Omega)^{1/2}]$ using a spin-up time scale based on the distance between the endwalls. The curves for the mixed time scale and spin-up time scale look identical, because they differ only by a constant for a single radius ratio.

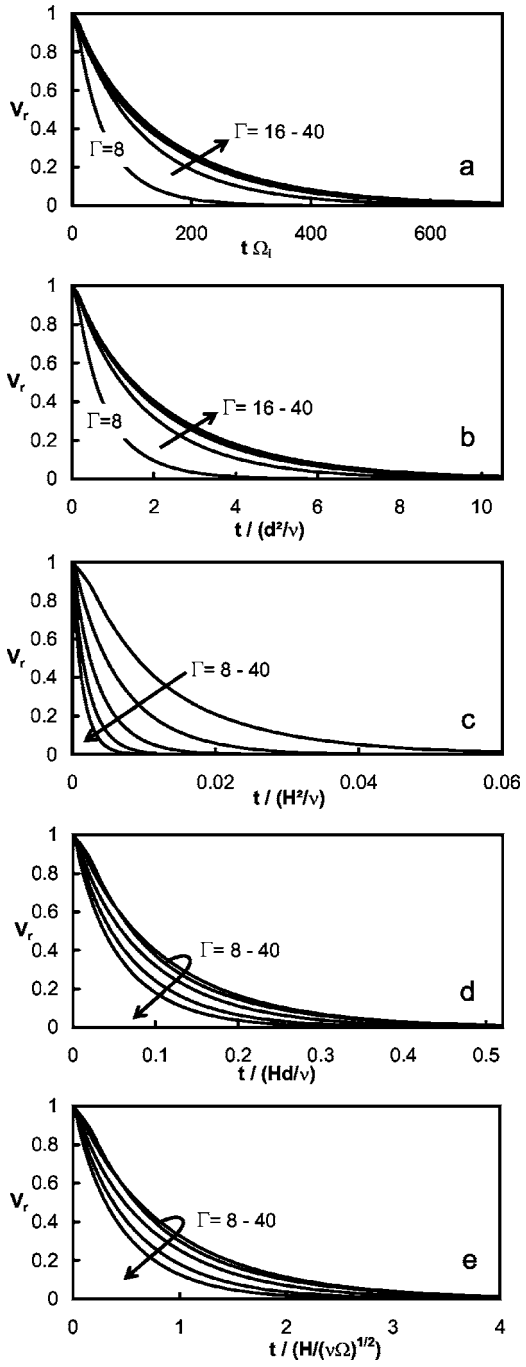

FIG. 3. Decay transient of the normalized maximum radial velocity for $\Gamma=8,16,24,32,40$ and $\eta=0.5$. The time scales in the individual plots are the same as Fig. 2.

tion. Nevertheless, this time scale collapses the data in the early portion of the transient for all aspect ratios. The collapse of data for early times but not for later times is again consistent with the idea of an early transient related to front propagation and a later transient related to phase diffusion for large aspect ratios.[33] Neither the mixed time scale, $\tau_{v,m}=Hd/\nu$, nor the spin-up time scale, $\tau_s=H/(\nu\Omega)^{1/2}$, collapse the data particularly well for the latter portion of the transient, as shown in Figs. 4(c) and 4(d). However, the mixed time scale provides the narrowest range of times, $0.4 \leqslant t/(Hd/\nu) \leqslant 0.85$, for vortical structure to reach 95% of its final value. While this range is fairly broad, the values are $O(1)$, unlike either of the other two viscous time scales, $\tau_{v,r}=d^2/\nu$ and $\tau_{v,z}=H^2/\nu$. The spin-up time scale also provides a time to reach 95% of the final value that is $O(1)$, but the range of values is much larger than that for the mixed time scale. The relatively narrow range of times to reach 95% of the final value and the time scale being $O(1)$ suggest

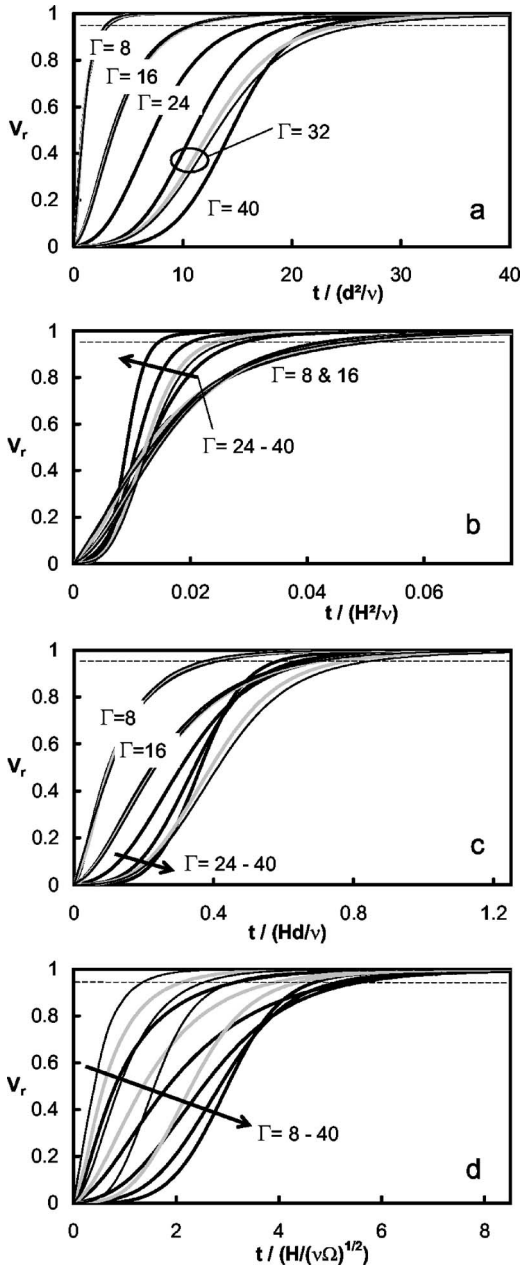

FIG. 4. Onset transient of the normalized maximum radial velocity for $\Gamma=8,16,24,32,40$ with $\eta=0.5$ (bold black), $\Gamma=8,16,32$ with $\eta=0.7$ (gray), and $\Gamma=8,16,32$ with $\eta=0.9$ (fine black). For easy comparison between the scales, the horizontal axis is adjusted so that the time to reach 95% of the final velocity for the longest duration for the onset is two-thirds of the entire horizontal extent of the plot in all cases. (a) Time is scaled as $t/(d^2/\nu)$ using a viscous time scale based on the gap between the cylinders; (b) time is scaled as $t/(H^2/\nu)$ using a viscous time scale based on the distance between the endwalls; (c) time is scaled as $t/(Hd/\nu)$ using a mixed viscous time scale; (d) time is scaled as $t/[H/(\nu\Omega)^{1/2}]$ using a spin-up time scale based on the distance between the endwalls. The horizontal dashed line is at 0.95 V_r.

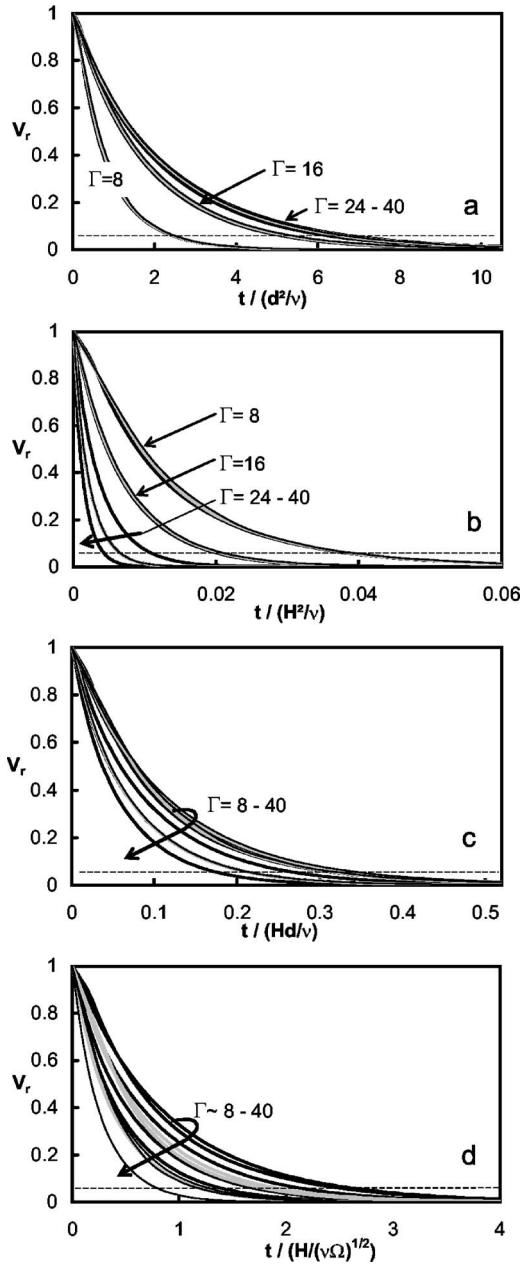

FIG. 5. Decay transient of the normalized maximum radial velocity for $\Gamma=8,16,24,32,40$ with $\eta=0.5$ (bold black), $\Gamma=8,16,32$ with $\eta=0.7$ (gray), and $\Gamma=8,16,32$ with $\eta=0.9$ (fine black). The time scales in the individual plots are the same as Fig. 4. The horizontal dashed line is at 0.05 V_r.

that the most appropriate physical time scale for the onset is Hd/ν. Thus, the onset of vortices is largely controlled by the endwalls through the Ekman vortex structure and its propagation as a front away from the endwalls.

The time scale for the decay of the Taylor vortex structure is substantially different, as is evident in Fig. 5. For the viscous time scale, $\tau_{v,r}=d^2/\nu$, the decay curves for the vortical structures nearly collapse [Fig. 5(a)] for $16\leqslant\Gamma\leqslant40$. The decay is faster for $\Gamma=8$, presumably due to the influence of the endwalls. None of the time scales based on the axial length of the annulus, H, collapse the curves, even if the $\Gamma=8$ case is omitted. Thus, the decay of the vortical structure is controlled by the viscous effects of the sidewalls of the cylinders, with corresponding length scale d. Furthermore, the time for the decay of Taylor vortices to only 5% of their initial value is $t/(d^2/\nu)\approx6$ for long cylinders ($\Gamma\geqslant16$), which is $O(1)$, as expected for a time scale relevant to the physics of the situation. The spin-up time scale is also $O(1)$, but the collapse of the data is clearly not as good as for $t/(d^2/\nu)$.

V. CONCLUSIONS

Although the time scale for the onset of the Taylor vortex structure cannot be predicted based on Taylor's original linear stability analysis, the computational "experiments" described here indicate that the time for the onset of vortices depends on the distance between the endwalls, except for infinitely long cylinders. This is clearly a consequence of the time for the vortical structure initiated as Ekman vortices by viscosity at the endwalls to propagate to the midlength of the annulus. On the other hand, decay of vortices results from the viscous damping of the sidewalls of the annulus.

Taylor-Couette flow experiments are often based on incrementally increasing or decreasing the rotation rate, but the time to wait for steady conditions is not clear. Although researchers have used a criterion based on $\tau_{v,r}=d^2/\nu$ or $\tau_{v,z}=H^2/\nu$, neither is correct for the onset of vortices, and only the first is correct for decay. We recommend that a time of about Hd/ν elapses before the flow is considered to be at steady state for the onset of vortices and that a time of about $10d^2/\nu$ elapses for the decay of vortices. Thus, the time for onset of the vortical structure is approximately 0.1Γ times the time for decay of the vortices, a ratio consistent with the results in Table I.

Finally, the time scales that we provide are for the transition from nonvortical to vortical structures and vice versa. The time scales to reach steady state when not transitioning from subcritical to supercritical flow or vice versa may be different. Likewise, the time scale for higher-order transitions such as onset of wavy vortex flow is still an open question.

ACKNOWLEDGMENTS

Thanks to the scientific committee of Centre National de la Recherche Scientifique (CNRS) computing center (IDRIS) for supporting this work. We are grateful for helpful discussions with Dr. Patrick Bontoux and Dr. Eric Serre of LMSNM, CNRS—Universités d'Aix-Marseille, France.

[1] G. Pfister and I. Rehberg, "Space-dependent order parameter in circular Couette flow transitions," Phys. Lett. **83A**, 19 (1981).
[2] G. Ahlers and D. S. Cannell, "Vortex-front propagation in rotating Couette-Taylor flow," Phys. Rev. Lett. **50**, 1583 (1983).
[3] M. Lücke, M. Mihelcic, and K. Wingerath, "Front propagation and pattern formation of Taylor vortices growing into unstable circular Couette flow," Phys. Rev. A **31**, 396 (1985).
[4] O. Czarny, E. Serre, P. Bontoux, and R. M. Lueptow, "Interaction between Ekman pumping and the centrifugal instability in Taylor-Couette flow," Phys. Fluids **15**, 467 (2003).
[5] T. B. Benjamin, "Bifurcation phenomena in steady flows of a viscous fluid. I: Theory," Proc. R. Soc. London, Ser. A **359**, 1 (1978).
[6] T. Alziary de Roquefort and G. Grillaud, "Computation of Taylor vortex flow by a transient implicit method," Comput. Fluids **6**, 259 (1978).
[7] D.-C. Kuo and K. S. Ball, "Taylor-Couette flow with buoyancy: Onset of spiral flow," Phys. Fluids **9**, 2872 (1997).
[8] V. Sobolik, B. Izrar, R. Lusseyran, and S. Skali, "Interaction between the Ekman layer and the Couette-Taylor instability," Int. J. Heat Mass Transfer **43**, 4381 (2000).
[9] J. Abshagen, O. Meincke, G. Pfister, K. A. Cliffe, and T. Mullin, "Transient dynamics at the onset of Taylor vortices," J. Fluid Mech. **476**, 335 (2003).
[10] J. E. Burkhalter and E. L. Koschmieder, "Steady supercritical Taylor vortex flow," J. Fluid Mech. **58**, 547 (1973).
[11] T. B. Benjamin, "Bifurcation phenomena in steady flows of a viscous fluid. II: Experiments," Proc. R. Soc. London, Ser. A **359**, 27 (1978).
[12] T. B. Benjamin and T. Mullin, "Anomalous modes in the Taylor experiment," Proc. R. Soc. London, Ser. A **377**, 221 (1981).
[13] K. A. Cliffe and T. Mullin, "A numerical and experimental study of anomalous modes in the Taylor experiment," J. Fluid Mech. **153**, 243 (1985).
[14] A. Lorenzen and T. Mullin, "Anomalous modes and finite-length effects in Taylor-Couette flow," Phys. Rev. A **31**, 3463 (1985).
[15] M. Niklas, M. Lücke, and H. Müller-Krumbhaar, "Velocity of a propagating Taylor-vortex front," Phys. Rev. A **40**, 493 (1989).
[16] H. A. Snyder, "Wave-number selection at finite amplitude in rotating Couette flow," J. Fluid Mech. **35**, 273 (1969).
[17] K. Park, G. L. Crawford, and R. J. Donnelly, "Determination of transition in Couette flow in finite geometries," Phys. Rev. Lett. **47**, 1448 (1981).
[18] G. P. Neitzel, "Numerical computation of time-dependent Taylor-vortex flows in finite-length geometries," J. Fluid Mech. **141**, 51 (1984).
[19] T. H. Squire, D. F. Jankowski, and G. P. Neitzel, "Experiments with deceleration from a Taylor-vortex flow," Phys. Fluids **29**, 2742 (1986).
[20] J. K. Koga and E. L. Koschmieder, "Taylor vortices in short fluid columns," Phys. Fluids A **1**, 1475 (1989).
[21] R. J. Weiner, P. W. Hammer, C. E. Swanson, and R. J. Donnelly, "Stability of Taylor-Couette flow subject to an external Coriolis force," Phys. Rev. Lett. **64**, 1115 (1990).
[22] P. W. Hammer, R. J. Weiner, and R. J. Donnelly, "Bifurcation phenomena in nonaxisymmetric Taylor-Couette flow," Phys. Rev. A **46**, 7578 (1992).
[23] E. Ikeda and T. Maxworthy, "Spatially forced corotating Taylor-Couette flow," Phys. Rev. E **49**, 5218 (1994).
[24] D. Hirshfeld and D. C. Rapaport, "Growth of Taylor vortices: A molecular dynamics study," Phys. Rev. E **61**, R21 (2000).
[25] Q. Xiao, T. T. Lim, and Y. T. Chew, "Second Taylor vortex flow: Effects of radius ratio and aspect ratio," Phys. Fluids **14**, 1537 (2002).
[26] B. Dubrulle, O. Dauchot, F. Daviaud, P.-Y. Longaretti, D. Richard, and J.-P. Zahn, "Stability and turbulent transport in Taylor-Couette flow from analysis of experimental data," Phys. Fluids **17**, 095103 (2005).
[27] R. C. DiPrima and H. L. Swinney, in *Topics in Applied Physics, Hydrodynamic Instabilities and the Transition to Turbulence*, edited by H. L. Swinney and J. P. Gollub (Springer-Verlag, Berlin, 1985), pp. 139–180.
[28] Y. Takeda, K. Kobashi, and W. E. Fischer, "Observation of the transient behaviour of Taylor vortex flow between rotating concentric cylinders after sudden start," Exp. Fluids **9**, 317 (1990).
[29] K. Park, G. L. Crawford, and R. J. Donnelly, "Characteristic lengths in the wavy vortex state of Taylor-Couette flow," Phys. Rev. Lett. **51**, 1352 (1983).
[30] G. P. King and H. L. Swinney, "Limits of stability and irregular flow patterns in wavy vortex flow," Phys. Rev. A **27**, 1240 (1983).
[31] S. T. Wereley and R. M. Lueptow, "Azimuthal velocity in supercritical circular Couette flow," Exp. Fluids **18**, 1 (1994).
[32] H. P. Greenspan, *The Theory of Rotating Fluids* (Cambridge University Press, London, 1969).
[33] P. Manneville, private Communication (2006). From numerical simulations, there are two stages to the onset transient based on the relaxation time of vortex wavelengths. The early stage of the onset transient is related to propagation of the front of the bifurcated state from the endwalls, while the late stage is related to slow wavelength adjustment related to phase diffusion for aspect ratios $\Gamma > 16$.
[34] E. Serre, E. Crespo del Arco, and P. Bontoux, "Annular and spiral patterns in flows between rotating and stationary discs," J. Fluid Mech. **434**, 65 (2001).
[35] O. Czarny, E. Serre, P. Bontoux, and R. M. Lueptow, "Interaction of wavy cylindrical Couette flow with the endwalls," Phys. Fluids **16**, 1140 (2004).
[36] J. M. Vanel, R. Peyret, and P. Bontoux, in *Numerical Methods for Fluid Dynamics II*, edited by K. W. Morton and M. J. Baines (Clarendon, Oxford, 1986), pp. 463–475.
[37] I. Raspo, S. Hughes, E. Serre, A. Randriamampianina, and P. Bontoux, "A spectral projection method for the simulation of complex three-dimensional rotating flows," Comput. Fluids **31**, 745 (2002).
[38] R. C. DiPrima, P. M. Eagles, and B. S. Ng, "The effect of radius ratio on the stability of Couette flow and Taylor vortex flow," Phys. Fluids **27**, 2403 (1984).
[39] A. Recktenwald, M. Lücke, and H. W. Müller, "Taylor vortex formation in axial through-flow: Linear and weakly nonlinear analysis," Phys. Rev. E **48**, 4444 (1993).